BIOCHEMISTRY
including biophysical chemistry & molecular biology

Article

pubs.acs.org/biochemistry

Plasmin Substrate Binding Site Cooperativity Guides the Design of Potent Peptide Aldehyde Inhibitors

Joakim E. Swedberg and Jonathan M. Harris*

Institute of Health and Biomedical Innovation, Queensland University of Technology, Brisbane, Queensland 4059, Australia

ABSTRACT: Perioperative bleeding is a cause of major blood loss and is associated with increased rates of postoperative morbidity and mortality. To combat this, antifibrinolytic inhibitors of the serine protease plasmin are commonly used to reduce bleeding during surgery. The most effective and previously widely used of these is the broad range serine protease inhibitor aprotinin. However, adverse clinical outcomes have led to use of alternative serine lysine analogues to inhibit plasmin. These compounds suffer from low selectivity and binding affinity. Consequently, a concerted effort to discover potent and selective plasmin inhibitors has developed. This study used a noncombinatorial peptide library to define plasmin's extended substrate specificity and guide the design of potent transition state analogue inhibitors. The various substrate binding sites of plasmin were found to exhibit a higher degree of cooperativity than had previously been appreciated. Peptide sequences capitalizing on these features produced high-affinity inhibitors of plasmin. The most potent of these, Lys-Met(sulfone)-Tyr-Arg-H [KM(O_2)YR-H], inhibited plasmin with a K_i of 3.1 nM while maintaining 25-fold selectivity over plasma kallikrein. Furthermore, 125 nM (0.16 μg/mL) KM(O_2)YR-H attenuated fibrinolysis in vitro with an efficacy similar to that of 15 nM (0.20 μg/mL) aprotinin. To date, this is the most potent peptide inhibitor of plasmin that exhibits selectivity against plasma kallikrein, making this compound an attractive candidate for further therapeutic development.

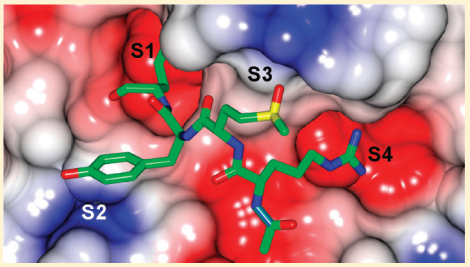

Perioperative bleeding is a significant cause of blood loss[1] and greatly contributes to postoperative complications.[2] Major blood loss necessitates transfusion, which is itself associated with risks of allergic reactions, mismatched transfusion, and transmission of infections.[3] Additionally, there is a global shortage of blood products.[4] Therefore, pharmacological intervention is commonly employed to reduce excessive bleeding and demand for blood transfusions during surgery, with antifibinolytic therapy being the most frequently employed strategy.[5]

The serine protease plasmin is the primary enzyme responsible for dissolution of fibrin,[6] the main structural component of blood clots. Commonly used antifibrinolytics inhibit plasmin directly by preventing activation of its zymogen, plasminogen. Zymogen processing primarily occurs through two activators, urokinase-type plasminogen activator (uPA)[7] and tissue-type plasminogen activator (tPA),[8] with tPA being considered the most physiologically relevant in the intravascular compartment. Plasminogen activation by tPA can occur at an appreciable rate only when both the zymogen and activator are bound to fibrin through lysine binding sites on their kringle domains,[9] thereby restricting plasmin activity to the area of clotting. Further regulation occurs both at the level of plasminogen activation by plasminogen activator inhibitor-1[10] or thrombin activatable fibrinolysis inhibitor[11] and at the level of plasmin, primarily by α-antiplasmin.[12]

Until recently, the plasmin inhibitor aprotinin (Trasylol) was both the most effective and widely used antifibinolytic for reduction of perioperative bleeding.[1] Aprotinin is a Kunitz-type serine protease inhibitor originally isolated from bovine lung tissue[13] that inhibits virtually all serine proteases.[14] However, use of aprotinin as an antifibrinolytic has been linked to increased incidence of myocardial infarction,[15] vein graft hypercoagulation,[16] and renal failure.[17,18] Accordingly, general use of aprotinin was discontinued in November 2007 after a large multicenter study from the Blood Conservation using Antifibrinolytics in a Randomized Trial found higher mortality rates associated with aprotinin compared to alternative treatments in the form of lysine analogues.[19]

ε-Aminocaprioic acid[20] and tranexamic acid[21] are lysine analogues that do not inhibit plasmin directly but rather bind to plasminogen's lysine binding sites, preventing binding to fibrin and therefore efficient conversion to plasmin.[22] Although they have previously been thought to have unproven efficacy in reducing bleeding during surgery,[23,24] there is a growing consensus suggesting that these compounds reduce the need for blood products. However, their reported level of effectiveness varies,[1,19,25−28] and both lysine analogues suffer from poor affinity requiring high doses (ε-aminocaprioic acid, 10−30 g; tranexamic acid, 3−10 g), with loading doses at induction of anesthesia that are equivalent to millimolar plasma concentrations.[23,28] Because these compounds inhibit any lysine domain binding interaction, high concentrations may result in clinical effects beyond plasmin inhibition and have been linked to nonischemic seizures.[28] Consequently, there is a need for development of more potent and specific inhibitors of

Received: August 3, 2011
Revised: August 29, 2011
Published: August 30, 2011

plasmin that can be administered at lower concentrations with a reduced risk of off-target effects.

As with any protease target, design of potent and selective small molecule inhibitors against plasmin requires detailed knowledge of the active site architecture and resulting substrate preference. The extended substrate specificity of plasmin has previously been investigated using positional-scanning synthetic combinatorial libraries (PS-SCL).[29−31] PS-SCL sublibraries are produced with mixtures of amino acids with differential reaction rates, and equal representation of all amino acids is unlikely,[32] causing a high level of variability and a lack of reproducibility. As a consequence, conflicting substrate preferences have been reported for plasmin, suggesting that the substrate specificity of this protease is yet to be fully defined. It has previously been shown that PS-SCL data may be deconvoluted by screening against a noncombinatorial peptide library that included preferred amino acid sequences from PS-SCLs.[34]

This study focuses on fully defining plasmin's extended substrate preference by screening against a noncombinatorial peptide substrate library using a *p*-nitroanilide (pNA) reporter group (λ_{max} = 405 nm). The peptide library screen revealed that a high degree of substrate binding subsite cooperativity existed for plasmin. Sequences of substrates cleaved with high efficiency were selected as candidates for plasmin peptide aldehyde transition state analogue inhibitors. The most potent of these, Ac-KM(O_2)YR-H, inhibited plasmin (K_i = 3.08 ± 0.26) with 25-fold selectivity over plasma kallikrein (pKLK). Furthermore, 0.16 μg/mL Ac-KM(O_2)YR-H prevented fibrinolysis with an efficacy similar to that of 0.20 μg/mL aprotinin in an in vitro fibrinolysis assay.

MATERIALS AND METHODS

Peptide Synthesis. All peptide synthesis reagents and solvents were of analytical grade and obtained from Auspep Pty Ltd. and Merck Pty Ltd., respectively, unless otherwise stated. Peptide *p*-nitroanilide (pNA) substrates were synthesized using *p*-phenylenediamine (Sigma-Aldrich) derivatized 2-chlorotrityl resin (1.3 mmol/g) as previously described.[33] Peptide elongation was performed with 4 equiv of 9-fluorenylmethyl carbamate-protected amino acids dissolved (0.25 M each) in 2-(1*H*-benzotriazol-1-yl)-1,1,3,3-tetramethyluronium hexafluorophosphate, 1-hydroxybenzotriazole, and *N*,*N*-diisopropylethylamine in *N*,*N*-dimethylformamide (DMF) for 1 h. Fmoc deprotection was achieved by treatment with 45% DMF, 50% piperidine, and 5% 1,8-diazabicyclo[5.4.0]undec-7-ene (Sigma-Aldrich) over a period of 10 min. Fully protected peptides were liberated from the solid support by successive changes of 1% trifluoroacetic acid (TFA) in dichloromethane (DCM) followed by ether precipitation and overnight oxidation using 8 equiv of Oxone (Sigma-Aldrich) in an acetonitrile/H_2O mixture (50:50). Protecting groups were removed from the dry product by cleavage for 2 h in 95% TFA, with scavengers: 1.25% triisopropylsilane (Sigma-Aldrich), 1.25% H_2O, and 2.5% thioanisole (Sigma-Aldrich). Peptides used for kinetic constants were purified by reverse phase high-performance liquid chromatography using a Jupiter 4 μm Proteo 90A C-18 column (Phenomenex) across a 20 to 100% 2-propanol/water gradient containing 0.1% TFA before mass validation using MALDI-TOF mass spectrometry (ProteinChip System, Bio-Rad), lyophilization, and storage at −20 °C.

Peptide aldehydes were synthesized on H-Arg(Boc)$_2$-H NovaSyn TG resin (0.21 mmol/g, Novabiochem) using coupling and deprotection conditions as described above. Side chain protecting groups were removed when the samples were washed with 5 volumes of TFA for 1 h before being washed three times with 10 volumes each of DCM, DMF, and acetonitrile to remove any residual TFA. Methionine was converted to methionine sulfone on resin by oxidation with Oxone (20 equiv) in a water/acetonitrile mixture (50:50) over 6 h before cleavage with 10 volumes of 1% TFA in a water/acetonitrile mixture (4:6). Peptide aldehydes were purified and validated as described above before being stored under a nitrogen atmosphere at −80 °C.

Kinetic Enzyme Assays. Lyophilized crude sparse matrix library (SML) peptide substrates were solubilized in 2-propanol and adjusted to equal molarity by total hydrolysis of the pNA moiety. Assays were performed with 6 nM human plasmin (Sigma-Aldrich) and approximately 133 μM peptide substrates (determined by total hydrolysis) in 300 μL of assay buffer [100 mM Tris-HCl (pH 8), 100 mM NaCl, and 0.005% Triton-X] containing 10% 2-propanol (from substrates), while hydrolysis was measured at 405 nM over 2 min at room temperature. Kinetic constants for selected peptide substrates (18.75−600 μM) were determined for plasmin (1 nM) and pKLK (2 nM) in 300 μL of assay buffer over 7 min and were calculated from three independent experiments by nonlinear regression using Prism 5 (GraphPad Software Inc.).

Inhibitor Assays. Increasing concentrations of inhibitors were assayed against various proteases (human plasmin, 1 nM; human thrombin, 50 nM; human pKLK, 2 nM; bovine β-trypsin, 1 nM; bovine α-chymotrypsin, 25 nM; recombinant human KLK4, 2 nM; human factor IXa, 20 nM; human factor XIa, 6 nM) as described above in 300 μL of assay buffer with 100 μM substrate over 7 min at room temperature. The assay buffers for trypsin and factor IXa also included 10 mM $CaCl_2$ with an additional 10% polyethylene glycol for factor IXa. Inhibition constants were determined from three independent experiments by nonlinear regression using Prism 5. Proteolysis assays were performed as described above with 7 μM human fibrinogen over 30 min (trypsin) or 90 min (plasmin) at 37 °C before termination by boiling in sodium dodecyl sulfate−polyacrylamide gel electrophoresis (SDS−PAGE) sample buffer. Proteolysis fragments were separated on 10% polyacrylamide gels and visualized by being stained with Coomassie brilliant blue R-250 (Sigma-Aldrich). All proteins excluding KLK4 were obtained from Sigma-Aldrich.

Protein Expression and Purification. Recombinant KLK4 was produced using an Sf9 insect cell expression construct as previously reported.[34,36] These expression vectors generate the complete KLK4 amino acid sequence followed by a V5 epitope (GKPIPNPLLGLDST) and polyhistidine tags. Pro-KLK4 was purified from conditioned media using Ni^{2+}-nitrilotriacetic acid agarose (Qiagen) according to the manufacturer's instructions. The identity of the expressed protein was confirmed by Western blot analysis before the zymogen was activated by incubation with thermolysin at a ratio of 1:40 for 60 min. Active KLK4 was purified in 50 mM Tris-HCl (pH 7.5) using a 1 mL Resource Q column (GE Healthcare) and eluted with 50 mM Tris-HCl (pH 7.5) and 0.5 M NaCl in a linear gradient before being stored at −80 °C

Fibrinolysis Assay. The fibrinolysis assay was performed as previously described[37] with the following changes. Increasing concentrations of inhibitor were mixed with plasmin and thrombin in 150 μL of fibrinolysis buffer [150 mM NaCl, 15 mM $CaCl_2$, and 100 mM Tris-HCl (pH 7.4)]. The assay was

initiated by the addition of fibrinogen in 50 μL of fibrinolysis buffer, and fibrin formation and degradation were monitored by absorbance at 400 nm over 3 h in a transparent 96-well microtiter plate. Final enzyme and substrate concentrations were 1.5 nM plasmin, 30 nM thrombin, and 4 mg/mL fibrinogen.

Molecular Modeling. Currently, there are no structural data for plasmin in a complex with an inhibitor. Accordingly, predictive molecular modeling was conducted using the catalytic domain of plasmin (μ-plasmin) using a μ-plasmin−streptokinase complex [Protein Data Bank (PDB) entry 1BML] as a template. Given the equivalent potency of the lead peptide inhibitors, we chose to model the Ac-RM(O_2)YR-H peptide aldehyde on the basis of its higher level of conformational restraint compared to that of Ac-KM(O_2)YR-H. The μ-plasmin−inhibitor [Ac-RM(O_2)YR-H] complex was produced by overlay of μ-plasmin and a trypsin−sunflower trypsin inhibitor (SFTI) complex (PDB entry 1SFI). Residues 2−5 of SFTI were substituted to generate an Ac-RM(O_2)YR-H−plasmin complex. All molecular modeling manipulations were conducted using YASARA Dynamics (version 10.7.8) and the AMBER03 force field.[38] Simulations were conducted at constant pressure and temperature, using the particle mesh Ewald algorithm for calculation of long-range electrostatics with nonbonded interactions truncated at 10.5 Å. μ-Plasmin (chain A) was solvated with TIP3P water (pH 8.0) and neutralized with Na^+Cl^- counterions to a final concentration of 100 mM. This generated a system of approximately 35000 atoms, including 10500 water molecules. The solvated μ-plasmin was subjected to conjugate gradient minimization before 100 ps molecular dynamics with fixed Cα atoms. After Cα atoms had been freed, a 500 ps molecular dynamics simulation was initiated, and an average simulation structure was determined.

RESULTS

Plasmin Substrate Binding Sites Show Strong Subsite Cooperativity. Plasmin's extended peptide substrate preference has previously been investigated using PS-SCL with conflicting results,[29−31] indicating that the substrate specificity of this protease is yet to be fully realized. Consequently, a noncombinatorial sparse matrix library (SML) of individually synthesized peptide substrates was designed to establish the most preferred plasmin peptide cleavage site. The SML incorporated amino acids that previous PS-SCL studies found to be preferred for the P1−P4 sites by plasmin and included basic P1 residues, aromatic P2 residues, polar P3 residues, and basic, hydrophobic, polar P4 residues (Table 1). Although Met is oxidized during synthesis of peptide-pNAs with the method used here,[33] the product Met sulfone [Met(O_2)/M(O_2)] appeared to fit plasmin's polar preference at the P3 site (rather than norleucine) and was consequently included.

Table 1. Design of a Sparse Matrix Library of Peptides

P1	P2	P3	P4	ref
K	W > F > Y	Q > A	K > R > Q > *F* > A	30
K	F > Y > W	T > n	K > n > V/F/I	29
K/R	F/Y/N	M/Q	not available	59
K/R	F/Y/W	M(O_2)/Q/T	K/R/M(O_2)/V/F	SML

Screening of the peptide library against plasmin (Figure 1) indicated that the preference for Lys over Arg at the P1 position was less pronounced than previously reported.[29,30] However, Lys at the P1 site did result in more promiscuous cleavage, while a slight preference for Tyr over Phe or Trp at the P2 site was apparent. Contrary to previous studies,[29,30] no clear preference for basic residues was observed at P4 when Lys occupied the P1 site. Indeed, five of the seven sequences hydrolyzed at the highest rate contained Phe or Val at this position. Placing Arg at the P1 site resulted in more restricted preferences at the other subsites, with reduced levels of cleavage of sequences having Trp at the P2 site in particular. Additionally, Met(O_2) and basic residues were relatively more favored at the P3 and P4 sites, respectively, when combined with Arg at the P1 site. These findings confirm the occurrence of cooperativity between the subsites of plasmin as has previously been suggested by a study using two PS-SCLs with either Arg or Lys at the P1 site.[31] As a consequence of plasmin subsite cooperativity, although substrates containing Lys at the P1 site were cleaved at a 43% higher rate on average, sequences cleaved with the highest rates were exclusively based on Arg at the P1 site.

Plasmin Cleaves Substrates with Arg at the P1 Site with the Highest Efficiency. Kinetic constants were determined for selected substrates to further guide the design of plasmin inhibitors. Sequences were chosen to provide a range of efficiencies (Table 2). Substrates with Arg rather than Lys at the P1 site were generally cleaved more efficiently as indicated by higher k_{cat}/K_M values. Indeed, the P1 Lys peptide with the highest k_{cat}/K_M [Ac-FM(O_2)YKpNA] was cleaved at only half the catalytic efficiency compared to that of the P1 Arg peptide with the highest k_{cat}/K_M [Ac-RM(O_2)YRpNA]. Contrary to previous findings,[29] it appeared that the P3 residue made a substantial contribution to the catalytic efficiency of cleavage because the k_{cat}/K_M values were considerably higher for all five sequences that included Met(O_2) at the P3 site. Overall, there was a high degree of correlation between the rates of hydrolysis from the SML screen and the k_{cat} values of the purified and mass-determined substrates. The sequence with the highest k_{cat}/K_M value [Ac-RM(O_2)YRpNA] was selected for use in all subsequent plasmin assays.

Previous PS-SCL studies[29−31] and the MEROPS peptidase database specificity matrixes (http://merops.sanger.ac.uk[39]) suggest that factor IXa and pKLK are the plasma proteases with the substrate preferences most similar to those of plasmin. Consequently, these proteases were used to evaluate the selectivity of substrate cleavage. pKLK showed a strong preference for Arg at P4 compared to Lys as shown by a k_{cat}/K_M ratio of 3.06 for Ac-RM(O_2)YRpNA and Ac-KM(O_2)-YRpNA while not appearing to have a particular partiality for any of the aromatic P2 residues (Table 2). The sequence Ac-KM(O_2)YRpNA appeared most selective for plasmin compared to pKLK as indicated by the highest k_{cat}/K_M ratio, while the substrate with the highest pKLK k_{cat}/K_M value (Ac-RQFRpNA) was used in subsequent assays for this enzyme. In contrast, neither of the peptide-pNAs assayed was cleaved by factor IXa (data not shown). These findings are contrary to a recent PS-SCL screen of factor IXa that indicated a substrate preference of Arg at P1, Phe/Tyr at P2, and Met/Glu at P3[31] and further highlight the need to verify results from PS-SCL screens using individually synthesized peptides. However, the substrate NGRpNA has previously been used as a factor IXa substrate,[40] and the QGRpNA sequence was readily hydrolyzed and used in subsequent factor IXa assays.

Peptide Aldehydes Based on Substrate Sequences Are Potent Plasmin Inhibitors. The sequences cleaved with

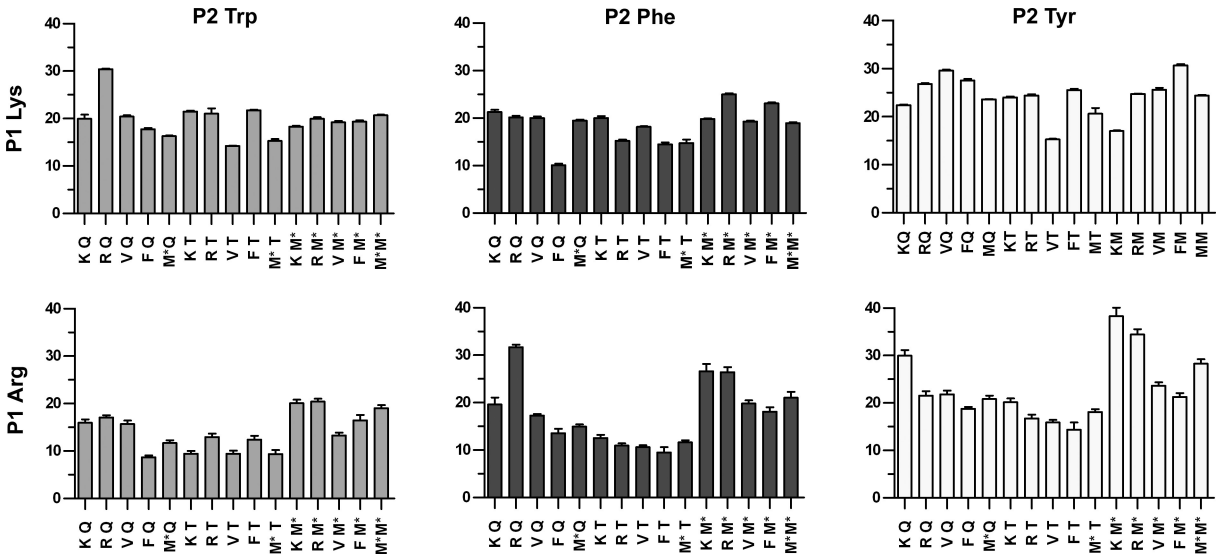

Figure 1. Amidolytic activity of plasmin against a sparse matrix library of peptide-pNA substrates. The *y*-axis represents the rate of plasmin substrate cleavage in milli-optical density units per minute at 405 nm. Amino acid sequences are labeled as follows: P1 residues, *y*-axis; P2 residues, *x*-axis above graphs; P4 and P3 residues, *x*-axis below graphs. Data are means ± the standard error of the mean from three independent experiments.

Table 2. Kinetic Constants of Peptide Substrates

enzyme	peptide substrate	expected mass	found mass	K_M (μM)	k_{cat} (s^{-1})	k_{cat}/K_M ($\times 10^4$ M^{-1} s^{-1})
plasmin	Ac-KM(O_2)YRpNA	790.99	791.78	61.28 ± 5.30	41.05 ± 0.29	66.99 ± 6.73
plasmin	Ac-RM(O_2)YRpNA	819.00	819.72	30.19 ± 1.22	30.45 ± 1.04	100.86 ± 1.01
plasmin	Ac-KM(O_2)FRpNA	774.99	776.07	42.57 ± 2.07	34.62 ± 0.44	81.32 ± 8.13
plasmin	Ac-VQYRpNA	726.94	728.01	109.1 ± 3.98	24.81 ± 0.32	22.74 ± 0.23
plasmin	Ac-RQFRpNA	767.94	769.07	64.28 ± 3.50	24.77 ± 0.40	38.53 ± 3.86
plasmin	Ac-RM(O_2)WRpNA	842.04	843.07	23.05 ± 1.82	20.57 ± 0.38	89.24 ± 8.92
plasmin	Ac-FM(O_2)YKpNA	781.98	782.97	63.39 ± 3.84	30.07 ± 0.54	48.43 ± 4.74
plasmin	Ac-RQWKpNA	778.96	780.11	99.05 ± 10.22	27.35 ± 0.96	27.60 ± 2.76
plasmin	Ac-KTFKpNA	684.89	685.94	236.20 ± 20.17	26.07 ± 0.99	11.04 ± 1.10
plasmin	Ac-VQYKpNA	698.87	699.79	136.20 ± 9.00	25.91 ± 0.64	19.02 ± 1.90
plasmin	Ac-KQWKpNA	750.95	752.27	85.57 ± 5.22	24.68 ± 0.49	28.84 ± 2.88
plasmin	Ac-FM(O_2)YKpNA	781.98	782.97	63.39 ± 3.84	30.07 ± 0.54	48.43 ± 4.74
pKLK	Ac-KM(O_2)YRpNA	–	–	361.20 ± 39.11	18.96 ± 1.05	5.25 ± 0.52
pKLK	Ac-RM(O_2)YRpNA	–	–	81.03 ± 4.34	13.01 ± 0.22	16.06 ± 1.61
pKLK	Ac-KM(O_2)FRpNA	–	–	267.00 ± 20.74	21.46 ± 0.77	8.04 ± 0.80
pKLK	Ac-VQYRpNA	–	–	69.28 ± 4.12	9.20 ± 0.17	13.28 ± 1.33
pKLK	Ac-RQFRpNA	–	–	87.12 ± 4.82	18.94 ± 0.34	21.74 ± 2.17

the highest k_{cat}/K_M [Ac-KM(O_2)YK, Ac-RM(O_2)YR, and Ac-KM(O_2)FR] were selected as candidates for plasmin peptide aldehyde inhibitors. Both Ac-KM(O_2)YK-H and Ac-RM(O_2)-YR-H inhibited plasmin effectively with K_i values of 3.08 and 9.9 nM, respectively, while Ac-KM(O_2)FR-H performed more poorly (Table 3). To determine the contribution from the various residues to binding affinity, peptide aldehydes Ac-KMYK-H, Ac-RMYK-H, Ac-M(O_2)YK-H, and Ac-MYR-H were also screened against plasmin. Replacing the P3 methionine sulfone with methionine or removing the P4 basic residues reduced the potency of inhibition of ∼10−30-fold, while both changes at once caused a 300-fold decrease in affinity. These findings suggest similar contributions from the P3 and P4 residues to binding affinity.

To assess the specificity of inhibition, we screened the most potent inhibitor Ac-KM(O_2)YK-H against trypsin, pKLK, thrombin, factor IXa, factor XIa, kallikrein-related peptidase 4, and α-chymotrypsin. Trypsin and pKLK were inhibited with K_i values of 95 and 366 nM, respectively. Some inhibition of factor IXa occurred above 5000 nM, with no inhibition of the other proteases tested up to 10000 nM. However, inhibition of cleavage of small colorimetric peptides does not always translate to inhibition of protein proteolysis.[34,35] Consequently, the potency and selectivity of the inhibitors were evaluated against the protein substrate fibrinogen. Plasmin digestion of fibrinogen was completely blocked at 250 nM Ac-KM(O_2)YK-H or Ac-RM(O_2)YR-H (Figure 2A), while neither inhibitor substantially inhibited trypsin fibrinogen digestion up to 5000 nM (Figure 2B). These observations align with previous findings for the sunflower trypsin inhibitor (SFTI-1) and engineered variants targeting KLK4, where amidolytic inhibition is not directly proportional to proteolytic inhibition,[34,35] and highlight the need to evaluate inhibition of protein proteolysis when determining protease inhibitor efficacy.

Peptide Aldehyde Inhibitors Block Fibrinolysis in Vitro. During fibrinolysis, plasmin degrades fibrin rather than its precursor, fibrinogen. Therefore, an in vitro fibrin formation and dissolution assay was used to determine the ability of Ac-

dx.doi.org/10.1021/bi201203y | *Biochemistry* 2011, 50, 8454−8462

Table 3. Kinetic Constants of Plasmin Inhibitors

enzyme	inhibitor	expected mass	found mass	IC_{50} (nM)	substrate (100 μM)	K_i (nM)
plasmin	Ac-KMYR-H	622.77	624.00	102.6 ± 8.4	Ac-RM(O_2)YRpNA	–
plasmin	Ac-RMYR-H	650.78	651.98	310.0 ± 8.8	Ac-RM(O_2)YRpNA	–
plasmin	Ac-M(O_2)YR-H	526.60	527.74	186.6 ± 17.7	Ac-RM(O_2)YRpNA	–
plasmin	Ac-MYR-H	494.60	495.32	2681 ± 272	Ac-RM(O_2)YRpNA	–
plasmin	Ac-KM(O_2)FR-H	638.77	639.62	108.1 ± 5.6	Ac-RM(O_2)YRpNA	–
plasmin	Ac-RM(O_2)YR-H	682.78	683.96	9.9 ± 1.1	Ac-RM(O_2)YRpNA	3.08 ± 0.26
plasmin	Ac-KM(O_2)YR-H	654.77	656.04	8.8 ± 0.6	Ac-RM(O_2)YRpNA	3.25 ± 0.25
plasmin	aprotinin	–	–	–	–	0.18 ± 0.06[49]
trypsin	Ac-KM(O_2)YR-H	–	–	95.0 ± 2.7	Bz-FVRpNA	–
trypsin	aprotinin	–	–	–	–	0.02 ± 0.003[49]
pKLK	Ac-KM(O_2)YR-H	–	–	366.1 ± 26.0	Ac-RQFRpNA	78.6 ± 7.3
pKLK	aprotinin	–	–	–	–	13.4 ± 2.4[49]
thrombin	Ac-KM(O_2)YR-H	–	–	>10000	Bz-FVRpNA	–
factor IXa	Ac-KM(O_2)YR-H	–	–	>10000	Ac-QGRpNA	–
factor IXa	aprotinin	–	–	>5000[49]	–	–
factor XIa	Ac-KM(O_2)YR-H	–	–	6150 ± 1610	Bz-FVRpNA	–
KLK4	Ac-KM(O_2)YR-H	–	–	>10000	Bz-FVRpNA	–
chymotrypsin	Ac-KM(O_2)YR-H	–	–	>10000	Bz-WpNA	–
chymotrypsin	aprotinin	–	–	–	–	1.3 ± 0.43 [49]

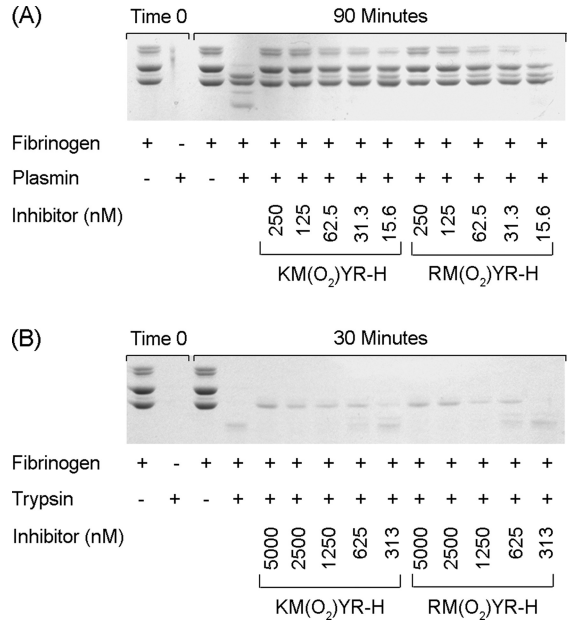

Figure 2. Inhibition of serine protease proteolytic activity by peptide aldehydes. Examination of fibrinogen proteolysis by plasmin and trypsin using SDS–PAGE. Inhibition of (A) plasmin and (B) trypsin in the presence of increasing concentrations of KM(O_2)YR-H and RM(O_2)YR-H. Bands were visualized with Coomassie blue staining after resolution on 10% polyacrylamide gels. Images are representative of three independent experiments.

KM(O_2)YK-H and Ac-RM(O_2)YR-H to impede fibrinolysis. Because fibrin is insoluble, its formation and degradation can be monitored by the scattering of light as previously described.[37] Similar methods have also been used to evaluate fibrinolysis and antifibinolytic compounds in human plasma.[41,42] The standard fibrinolysis inhibitor aprotinin was used as a benchmark for inhibition efficacy. Complete attenuation of fibrinolysis was achieved using either aldehyde inhibitor at 250 nM, which is equivalent to 0.164 and 0.171 μg/mL for Ac-KM(O_2)YK-H and Ac-RM(O_2)YR-H, respectively (Figure 3A,B). In the case of aprotinin, 31.25 nM or 0.204 μg/mL inhibitor was required to attain the same effect seen for the peptide aldehydes (Figure 3C).

Molecular Modeling of the Plasmin–Ac-RM(O_2)YR-H Complex. A model of μ-plasmin and Ac-RM(O_2)YR-H was generated by overlaying the trypsin–SFTI complex and μ-plasmin (rmsd of 0.86 Å over 204 Cα atoms) to position the inhibitor at the active site of plasmin (Figure 4A). The μ-plasmin–Ac-RM(O_2)YR-H modeled complex suggested that the protease–inhibitor interactions mainly involved hydrogen bonds rather than hydrophobic effects and exclusion of water. Surprisingly, there was no extended β-sheet formed at the interface between RM(O_2)YR-H and plasmin as is characteristic of many serine protease–inhibitor or –substrate complexes. While the uncertainties inherent in molecular modeling must be acknowledged, the observation is given weight by the existence of a similar arrangement for the complex formed between two other kringle domain proteases: thrombin with the Kunitz inhibitor boophilin[43] and hepatocyte growth factor activating protease with hepatocyte growth factor activating inhibitor-1.[44] The electronegative S1 pocket of plasmin generously accommodated Arg_4 of the inhibitor, with the guanidino group donating hydrogen bonds to the backbone carbonyl oxygens of Ser_{770} (Ser_{190}, trypsin residues and numbering), K_{770} (K_{224}), and P_{771} (P225) (Figure 4B,C). Plasmin's S2 pocket with the catalytic His_{603} (His_{57}) at the base allowed for π–π interactions with Tyr_3 in addition to the hydroxyl oxygen of the Tyr side chain donating a hydrogen bond to the oxygen of Gln_{738} (Gln_{192}). The S3 pocket of plasmin was electropositive as a result of the Arg_{719} (Gln_{175}) guanidino group, which donated a hydrogen bond to the Met_2 sulfone oxygen. This interaction was further stabilized by an intramolecular hydrogen bond between the other remaining Met_2 sulfone oxygen and the Met_2 backbone amine. In plasmin's electronegative S4 pocket, Arg_1 of Ac-RM(O_2)YR-H donated hydrogen bonds to both side chain oxygens of Glu_{724} (M_{180}), in addition to the backbone carbonyl oxygen of Arg_{719} (Gln_{175}).

dx.doi.org/10.1021/bi201203y | Biochemistry 2011, 50, 8454–8462

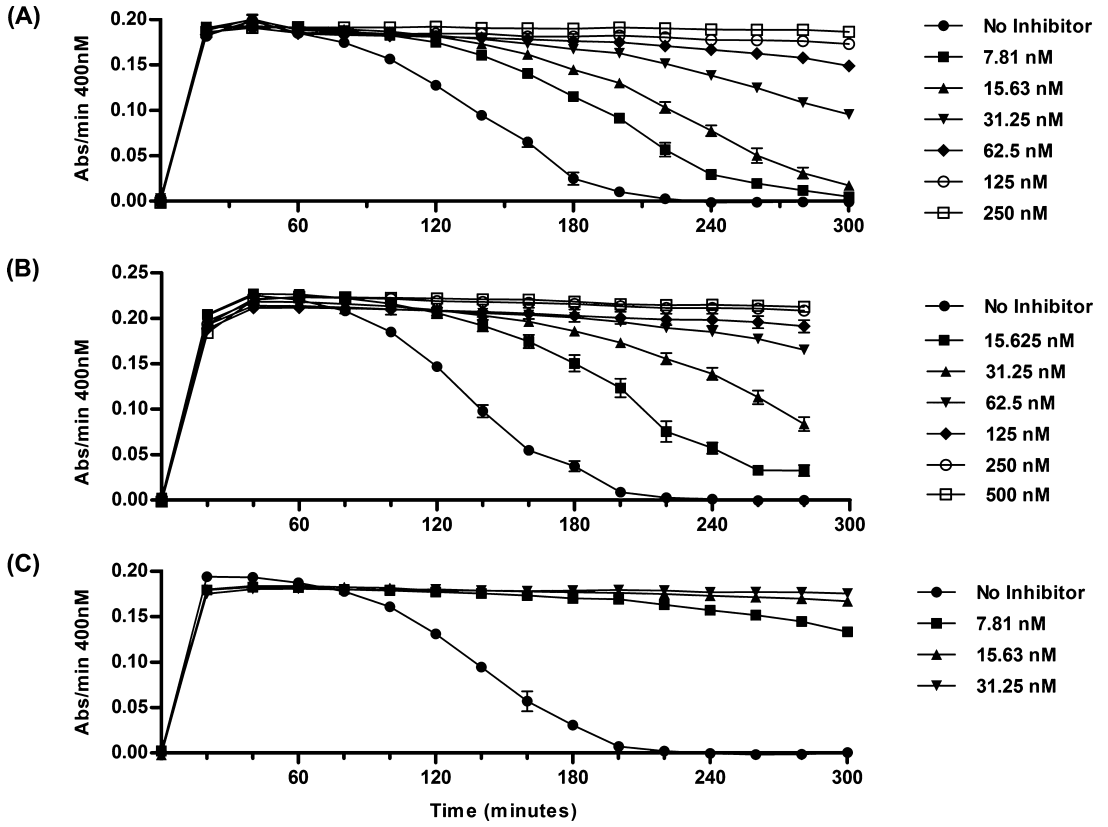

Figure 3. Inhibition of plasmin fibrinolysis *in vitro* by peptide aldehyde inhibitors. Formation of fibrin by thrombin and subsequent degradation by plasmin were monitored at 400 nm over 3 h. The ability of peptide aldehyde inhibitors to prevent fibrinolysis was assessed using various inhibitor concentrations of (A) KM(O_2)YR-H (0−250 nM), (B) RM(O_2)YR-H (0−500 nM), and (C) aprotinin (0−31.25 nM). Data are means ± the standard error of the mean from three independent experiments.

■ DISCUSSION

This study has further defined plasmin's extended peptide substrate specificity and has shown that cooperativity occurs between the enzyme's substrate binding subsites. Highly preferred peptide cleavage sequences that incorporated these features were used as templates to produce potent peptide aldehyde inhibitors of plasmin. The resulting inhibitors attenuated fibrinolysis in vitro with an efficacy comparable to that of aprotinin, making them attractive candidates for further therapeutic development.

Other studies that investigated plasmin's peptide substrate specificity have focused on screening combinatorial peptide libraries containing pools of peptides, without fully validating the results using individually synthesized substrates.[29−31] It has previously been shown that although PS-SCL gives a general indication of enzyme subsite preferences, optimal peptide sequences may be overlooked using this method.[34,45] This shortcoming in the PS-SCL screening method may be resolved by screening against a noncombinatorial SML of peptides more suited to revealing potential cooperativity between various substrate binding sites.[34,46] Applying this technique to plasmin resulted in the identification of highly preferred substrates that could not have been deduced by combinatorial library screening alone. This is particularly important when designing peptide or peptide mimetic protease inhibitors because optimal contact across all substrate binding sites is more likely to produce potent and selective inhibitors.

Currently, clinically available antifibrinolytics in the form of lysine analogues are nonspecific and low-affinity plasmin inhibitors. These are commonly administered using 1−15 g loading doses at induction of anesthesia,[1] which is equivalent to ∼0.4−6 mg/mL or ∼0.3−46 mM in plasma for an individual with an average blood volume of 4.5 L and a plasma content of 55%.[47] In comparison, a recommended loading dose of aprotinin has been estimated to be 280 mg or 0.11 mg/mL plasma with an optional pump priming dose of an additional 280 mg[1] or 0.11 mg/mL plasma, totaling a plasma concentration of 0.475 μM. This correlates well with in vitro plasma fibrinolysis assays for aprotinin in which 0.3 μM inhibitor completely blocks fibrinolysis.[42] In contrast, 100 μM tranexamic acid is needed in the same assay to achieve an equivalent level of inhibition, a concentration that is 333 times higher than that required for aprotinin. The most potent inhibitors in this study prevented in vitro fibrinolysis at a level comparable to that of aprotinin when used at an 8-fold higher molar concentration equating to a lower weight-to-volume concentration. However, relative efficacy does not always translate directly from an in vitro fibrinolysis assay to in vivo bleeding time reduction,[42] and the plasmin peptide aldehyde inhibitors require further in vivo testing to evaluate an effective dosing range.

Because plasminogen circulates at a concentration of 2 μM,[48] even potent inhibitors need to be administered at a concentration considerably higher than the inhibition constant (aprotinin K_i = 0.18 nM[49]). This presents a particular challenge in terms of achieving specificity of inhibition over other serine proteases present in plasma. The most potent inhibitor from this study is also likely to result in partial inhibition of pKLK if

dx.doi.org/10.1021/bi201203y | *Biochemistry* 2011, 50, 8454−8462

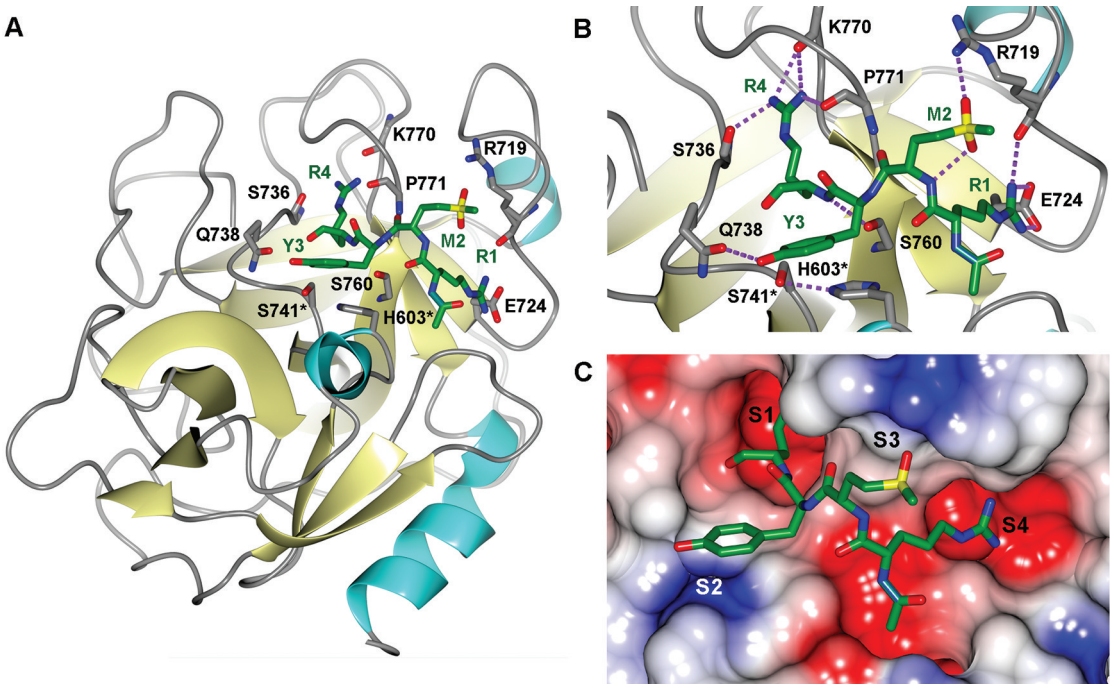

Figure 4. Structural characteristics of modeled protease−inhibitor interfaces of plasmin and Ac-RM(O_2)YR-H. (A) Ribbon plot of plasmin showing the bound peptide inhibitor RM(O_2)YR-H in stick model [carbon colored green (inhibitor) or gray (plasmin), oxygen colored red, nitrogen colored blue, and sulfur colored yellow, with hydrogen excluded]. Labels show residue type and number for plasmin (black) and RM(O_2)YR-H (green). (B) Close up of panel A showing hydrogen bonds (dashed purple lines) stabilizing the plasmin−inhibitor complex. (C) Molecular surface of plasmin with the bound inhibitor. Coloring is according to electrostatic potential (red indicates negative and blue positive), while substrate binding sites are labeled S1−S4.

it is administered at a dose required for appreciable in vivo reduction of blood loss. However, pKLK has a central role in initiation of the contact activation pathway,[50,51] and activation of the kallikrein−kinin system produces an elevated level of brandykin release, resulting in complement and neutrophil activation.[52,53] This is particularly important during cardiopulmonary bypass (CPB) surgery where contact with the artificial surfaces of the heart−lung machine initiates the contact pathway and systemic inflammatory response, a major contributor to organ damage during CPB.[53−55] Consequently, it has previously been suggested that dual inhibition of plasmin and pKLK may be desirable for an antifibrinolytic agent to be used during CPB procedures.[56]

However, nonspecific inhibitors have an inherent disadvantage because interaction with several physiological components is more likely to produce further variability in response across a diverse population of individuals. Therefore, the availability of individual specific regulators of coagulation, complement activation, and fibrinolysis would be ideal as it would allow for tailored treatment of different individuals. One way of increasing the specificity of inhibitors described in this study involves engagement of the prime side substrate binding sites (S′) of plasmin. Boronic acid inhibitors allow for contact at the protease prime side in addition to the nonprimed side and have recently been used to increase the potency of inhibition of kallikrein-related peptidase 3 (KLK3/PSA) more than 100-fold compared with that of the corresponding peptide aldehyde.[57] A recent study indicates that plasmin has a preference at the S2′ site for basic residues that is unique among the serine proteases within the circulatory system.[58] Consequently, combining the high-affinity plasmin P1−P4 sequences presented here with a P2′ basic residue using boronic acid as the transition state analogue may well produce a second generation of more potent and selective plasmin inhibitors.

In conclusion, this study has shown that although PS-SCL screening is an essential tool when defining protease substrate specificity, subsequent deconvolution of the results using an SML is needed to harness the full potential of PS-SCL. Bringing these two methods together identified substrate sequences cleaved with optimal catalytic efficiency and resulted in some of the most potent small molecule plasmin inhibitors produced to date.

AUTHOR INFORMATION

Corresponding Author

*E-mail: j2.harris@qut.edu.au. Phone: +61 (7) 3138 6186. Fax: + 61 (7) 3138 6030.

ABBREVIATIONS

uPA, urokinase-type plasminogen activator; tPA, tissue-type plasminogen activator; PS-SCL, positional-scanning synthetic combinatorial libraries; pNA, *p*-nitroanilide; pKLK, plasma kallikrein; DMF, *N*,*N*-dimethylformamide; TFA, trifluoroacetic acid; DCM, dichloromethane; Fmoc, fluorenylmethyloxycarbonyl; MALDI-TOF, matrix-assisted laser desorption ionization time-of-flight; Boc, di-*tert*-butyl dicarbonate; SML, sparse matrix library; KLK4, kallikrein-related peptidase 4; M(O_2) or Met(O_2), methionine sulfone; SFTI, sunflower trypsin inhibitor; Ac, acetyl group; Bz, benzyl group; rmsd, root-mean-square deviation; CPB, cardiopulmonary bypass; KLK3/PSA, kallikrein-related peptidase 3.

REFERENCES

(1) Mannucci, P. M., and Levi, M. (2007) Prevention and treatment of major blood loss. *N. Engl. J. Med. 356*, 2301−2311.

(2) Koh, M. B., and Hunt, B. J. (2003) The management of perioperative bleeding. *Blood Rev. 17*, 179−185.

(3) Blajchman, M. A., and Vamvakas, E. C. (2006) The continuing risk of transfusion-transmitted infections. *N. Engl. J. Med. 355*, 1303−1305.

(4) Goodnough, L.T., and Shander, A. (2007) Blood management. *Arch. Pathol. Lab. Med. 131*, 695−701.

(5) Levy, J. H. (2008) Pharmacologic methods to reduce perioperative bleeding. *Transfusion 48*, 31S−38S.

(6) Rijken, D. C., and Lijnen, H. R. (2009) New insights into the molecular mechanisms of the fibrinolytic system. *J. Thromb. Haemostasis 7*, 4−13.

(7) Robbins, K. C., Summaria, L., Hsieh, B., and Shah, R. J. (1967) The peptide chains of human plasmin. Mechanism of activation of human plasminogen to plasmin. *J. Biol. Chem. 242*, 2333−2342.

(8) Hoylaerts, M., Rijken, D. C., Lijnen, H. R., and Collen, D. (1982) Kinetics of the activation of plasminogen by human tissue plasminogen activator. Role of fibrin. *J. Biol. Chem. 257*, 2912−2919.

(9) Lerch, P. G., Rickli, E. E., Lergier, W., and Gillessen, D. (1980) Localization of individual lysine-binding regions in human plasminogen and investigations on their complex-forming properties. *Eur. J. Biochem. 107*, 7−13.

(10) Carmeliet, P., Bouche, A., De Clercq, C., Janssen, S., Pollefeyt, S., Wyns, S., Mulligan, R. C., and Collen, D. (1995) Biological effects of disruption of the tissue-type plasminogen activator, urokinase-type plasminogen activator, and plasminogen activator inhibitor-1 genes in mice. *Ann. N.Y. Acad. Sci. 748*, 367−381, 381−382 (discussion).

(11) Bajzar, L., Manuel, R., and Nesheim, M. E. (1995) Purification and characterization of TAFI, a thrombin-activable fibrinolysis inhibitor. *J. Biol. Chem. 270*, 14477−14484.

(12) Aoki, N., Moroi, M., and Tachiya, K. (1978) Effects of α2-plasmin inhibitor on fibrin clot lysis. Its comparison with α2-macroglobulin. *Thromb. Haemostasis 39*, 22−31.

(13) Kunitz, M., and Northrop, J. H. (1936) Isolation from beef pancreas of crystalline trypsinogen, trypsin, a trypsin inhibitor, and an inhibitor-trypsin compound. *J. Gen. Physiol. 19*, 991−1007.

(14) Ascenzi, P., Bocedi, A., Bolognesi, M., Spallarossa, A., Coletta, M., De Cristofaro, R., and Menegatti, E. (2003) The bovine basic pancreatic trypsin inhibitor (Kunitz inhibitor): A milestone protein. *Curr. Protein Pept. Sci. 4*, 231−251.

(15) Bukhari, E. A., Krukenkamp, I. B., Burns, P. G., Gaudette, G. R., Schulman, J. J., al-Fagih, M. R., and Levitsky, S. (1995) Does aprotinin increase the myocardial damage in the setting of ischemia and preconditioning? *Ann. Thorac. Surg. 60*, 307−310.

(16) Cosgrove, D. M. III, Heric, B., Lytle, B. W., Taylor, P. C., Novoa, R., Golding, L. A., Stewart, R. W., McCarthy, P. M., and Loop, F. D. (1992) Aprotinin therapy for reoperative myocardial revascularization: A placebo-controlled study. *Ann. Thorac. Surg. 54*, 1031−1036.

(17) Mangano, D. T., Tudor, I. C., and Dietzel, C. (2006) The risk associated with aprotinin in cardiac surgery. *N. Engl. J. Med. 354*, 353−365.

(18) Shaw, A. D., Stafford-Smith, M., White, W. D., Phillips-Bute, B., Swaminathan, M., Milano, C., Welsby, I. J., Aronson, S., Mathew, J. P., Peterson, E. D., and Newman, M. F. (2008) The effect of aprotinin on outcome after coronary-artery bypass grafting. *N. Engl. J. Med. 358*, 784−793.

(19) Fergusson, D. A., Hebert, P. C., Mazer, C. D., Fremes, S., MacAdams, C., Murkin, J. M., Teoh, K., Duke, P. C., Arellano, R., Blajchman, M. A., Bussieres, J. S., Cote, D., Karski, J., Martineau, R., Robblee, J. A., Rodger, M., Wells, G., Clinch, J., and Pretorius, R. (2008) A comparison of aprotinin and lysine analogues in high-risk cardiac surgery. *N. Engl. J. Med. 358*, 2319−2331.

(20) Okamoto, S., Nakajima, T., Okamoto, U., Watanabe, H., Iguchi, Y., Igawa, T., Chien, C., and Hayashi, T. (1959) A suppressing effect of ϵ-amino-N-caproic acid on the bleeding of dogs, produced with the activation of plasmin in the circulatory blood. *Keio J. Med. 8*, 247.

(21) Okamoto, S., Sato, S., Tanaka, Y., and Okamoto, U. (1964) An active sterioisomer (trans-form) of amcha and its and its and its antifibinolytic (antiplasmic) action *in vitro* and *in vivo*. *Keio J. Med. 13*, 177−185.

(22) Lucas, M. A., Fretto, L. J., and McKee, P. A. (1983) The relationship of fibrinogen structure to plasminogen activation and plasmin activity during fibrinolysis. *Ann. N.Y. Acad. Sci. 408*, 71−91.

(23) Royston, D. (1998) Aprotinin versus lysine analogues: The debate continues. *Ann. Thorac. Surg. 65*, 9−19.

(24) Carless, P. A., Moxey, A. J., Stokes, B. J., and Henry, D. A. (2005) Are antifibrinolytic drugs equivalent in reducing blood loss and transfusion in cardiac surgery? A meta-analysis of randomized head-to-head trials. *BMC Cardiovasc. Disord. 5*, 19−30.

(25) Kagoma, Y. K., Crowther, M. A., Douketis, J., Bhandari, M., Eikelboom, J., and Lim, W. (2009) Use of antifibrinolytic therapy to reduce transfusion in patients undergoing orthopedic surgery: A systematic review of randomized trials. *Thromb. Res. 123*, 687−696.

(26) Brown, J. R., Birkmeyer, N. J., and O'Connor, G. T. (2007) Meta-analysis comparing the effectiveness and adverse outcomes of antifibrinolytic agents in cardiac surgery. *Circulation 115*, 2801−2813.

(27) Henry, D., Carless, P., Fergusson, D., and Laupacis, A. (2009) The safety of aprotinin and lysine-derived antifibrinolytic drugs in cardiac surgery: A meta-analysis. *Can. Med. Assoc. J. 180*, 183−193.

(28) Koster, A., and Schirmer, U. (2010) Re-evaluation of the role of antifibrinolytic therapy with lysine analogs during cardiac surgery in the post aprotinin era. *Curr. Opin. Anaesthesiol. 24*, 92−97.

(29) Backes, B. J., Harris, J. L., Leonetti, F., Craik, C. S., and Ellman, J. A. (2000) Synthesis of positional-scanning libraries of fluorogenic peptide substrates to define the extended substrate specificity of plasmin and thrombin. *Nat. Biotechnol. 18*, 187−193.

(30) Harris, J. L., Backes, B. J., Leonetti, F., Mahrus, S., Ellman, J. A., and Craik, C. S. (2000) Rapid and general profiling of protease specificity by using combinatorial fluorogenic substrate libraries. *Proc. Natl. Acad. Sci. U.S.A. 97*, 7754−7759.

(31) Gosalia, D. N., Salisbury, C. M., Ellman, J. A., and Diamond, S. L. (2005) High throughput substrate specificity profiling of serine and cysteine proteases using solution-phase fluorogenic peptide microarrays. *Mol. Cell. Proteomics 4*, 626−636.

(32) Boutin, J. A., Gesson, I., Henlin, J. M., Bertin, S., Lambert, P. H., Volland, J. P., and Fauchere, J. L. (1997) Limitations of the coupling of amino acid mixtures for the preparation of equimolar peptide libraries. *Mol. Diversity 3*, 43−60.

(33) Abbenante, G., Leung, D., Bond, T., and Fairlie, D. P. (2000) An efficient Fmoc strategy for the rapid synthesis of peptide para-nitroanilides. *Lett. Pept. Sci. 7*, 347−351.

(34) Swedberg, J. E., Nigon, L. V., Reid, J. C., de Veer, S. J., Walpole, C. M., Stephens, C. R., Walsh, T. P., Takayama, T. K., Hooper, J. D., Clements, J. A., Buckle, A. M., and Harris, J. M. (2009) Substrate-guided design of a potent and selective kallikrein-related peptidase inhibitor for kallikrein 4. *Chem. Biol. 16*, 633−643.

(35) Swedberg, J. E., de Veer, S. J., Sit, K. C., Reboul, C. F., Buckle, A. M., and Harris, J. M. (2011) Mastering the canonical loop of serine protease inhibitors: enhancing potency by optimising the internal hydrogen bond network. *PLoS One 6*, e19302.

(36) Ramsay, A. J., Dong, Y., Hunt, M. L., Linn, M., Samaratunga, H., Clements, J. A., and Hooper, J. D. (2008) Kallikrein-related peptidase 4 (KLK4) initiates intracellular signaling via protease-activated receptors (PARs). KLK4 and PAR-2 are co-expressed during prostate cancer progression. *J. Biol. Chem. 283*, 12293−12304.

(37) Wolberg, A. S., Gabriel, D. A., and Hoffman, M. (2002) Analyzing fibrin clot structure using a microplate reader. *Blood Coagulation Fibrinolysis 13*, 533−539.

(38) Duan, Y., Wu, C., Chowdhury, S., Lee, M. C., Xiong, G., Zhang, W., Yang, R., Cieplak, P., Luo, R., Lee, T., Caldwell, J., Wang, J., and Kollman, P. (2003) A point-charge force field for molecular mechanics simulations of proteins based on condensed-phase quantum mechanical calculations. *J. Comput. Chem. 24*, 1999−2012.

(39) Rawlings, N.D. (2009) A large and accurate collection of peptidase cleavages in the MEROPS database. *Database (Oxford) 2009*, bap015.
(40) Yang, L., Gopalakrishna, K., Manithody, C., and Rezaie, A. R. (2006) Expression, purification and characterization of factor IX derivatives using a novel vector system. *Protein Expression Purif. 50*, 196−202.
(41) Kim, P. Y., Stewart, R. J., Lipson, S. M., and Nesheim, M. E. (2007) The relative kinetics of clotting and lysis provide a biochemical rationale for the correlation between elevated fibrinogen and cardiovascular disease. *J. Thromb. Haemostasis 5*, 1250−1256.
(42) Sperzel, M., and Huetter, J. (2007) Evaluation of aprotinin and tranexamic acid in different in vitro and in vivo models of fibrinolysis, coagulation and thrombus formation. *J. Thromb. Haemostasis 5*, 2113−2118.
(43) Macedo-Ribeiro, S., Almeida, C., Calisto, B. M., Friedrich, T., Mentele, R., Sturzebecher, J., Fuentes-Prior, P., and Pereira, P. J. (2008) Isolation, cloning and structural characterisation of boophilin, a multifunctional Kunitz-type proteinase inhibitor from the cattle tick. *PLoS One 3*, e1624.
(44) Eigenbrot, C., Ganesan, R., and Kirchhofer, D. (2010) Hepatocyte growth factor activator (HGFA): Molecular structure and interactions with HGFA inhibitor-1 (HAI-1). *FEBS J. 277*, 2215−2222.
(45) Schneider, E. L., and Craik, C. S. (2009) Positional scanning synthetic combinatorial libraries for substrate profiling. *Methods Mol. Biol. 539*, 59−78.
(46) Swedberg, J. E., de Veer, S. J., and Harris, J. M. (2010) Natural and engineered kallikrein inhibitors: An emerging pharmacopoeia. *Biol. Chem. 391*, 357−374.
(47) Tietz, N. W. (1995) *Clinical guide to laboratory tests*, 3rd ed., W. B. Saunders, Philadelphia.
(48) Collen, D., and Lijnen, H. R. (1991) Basic and clinical aspects of fibrinolysis and thrombolysis. *Blood 78*, 3114−3124.
(49) Delaria, K.A., Muller, D. K., Marlor, C. W., Brown, J. E., Das, R. C., Roczniak, S. O., and Tamburini, P. P. (1997) Characterization of placental bikunin, a novel human serine protease inhibitor. *J. Biol. Chem. 272*, 12209−12214.
(50) Campbell, D.J. (2001) The kallikrein-kinin system in humans. *Clin. Exp. Pharmacol. Physiol. 28*, 1060−1065.
(51) Colman, R. W., and Schmaier, A. H. (1997) Contact system: A vascular biology modulator with anticoagulant, profibrinolytic, antiadhesive, and proinflammatory attributes. *Blood 90*, 3819−3843.
(52) Wachtfogel, Y. T., Kucich, U., Hack, C. E., Gluszko, P., Niewiarowski, S., Colman, R. W., and Edmunds, L. H. Jr. (1993) Aprotinin inhibits the contact, neutrophil, and platelet activation systems during simulated extracorporeal perfusion. *J. Thorac. Cardiovasc. Surg. 106*, 1−9, , 9−10 (discussion).
(53) McEvoy, M.D., Reeves, S. T., Reves, J. G., and Spinale, F. G. (2007) Aprotinin in cardiac surgery: A review of conventional and novel mechanisms of action. *Anesth. Analg. (Hagerstown, MD, U.S.) 105*, 949−962.
(54) Levy, J. H., and Tanaka, K. A. (2003) Inflammatory response to cardiopulmonary bypass. *Ann. Thorac. Surg. 75*, S715−S720.
(55) Rubens, F. D., and Mesana, T. (2004) The inflammatory response to cardiopulmonary bypass: A therapeutic overview. *Perfusion 19*, 5−12.
(56) Dietrich, W., Nicklisch, S., Koster, A., Spannagl, M., Giersiefen, H., and van de Locht, A. (2009) CU-2010: A novel small molecule protease inhibitor with antifibrinolytic and anticoagulant properties. *Anesthesiology 110*, 123−130.
(57) LeBeau, A. M., Singh, P., Isaacs, J. T., and Denmeade, S. R. (2008) Potent and selective peptidyl boronic acid inhibitors of the serine protease prostate-specific antigen. *Chem. Biol. 15*, 665−674.
(58) Bajaj, M. S., Ogueli, G. I., Kumar, Y., Vadivel, K., Lawson, G., Shanker, S., Schmidt, A. E., and Bajaj, S. P. (2011) Engineering Kunitz domain 1 (KD1) of human tissue factor pathway inhibitor-2 to selectively inhibit fibrinolysis: Properties of KD1-L17R variant. *J. Biol. Chem. 286*, 4329−4340.
(59) Gosalia, D. N., Salisbury, C. M., Maly, D. J., Ellman, J. A., and Diamond, S. L. (2005) Profiling serine protease substrate specificity with solution phase fluorogenic peptide microarrays. *Proteomics 5*, 1292−1298.